DOI: 10.17344/acsi.2019.5784 *Acta Chim. Slov.* **2020,** *67,* 822–829

Scientific paper

Structural Diversity in Oxadiazole-Containing Silver Complexes Dependent on the Anions

Long Zhao,[†1] Long-Yan Xie,[†1] Xiu-Li Du,[†1] Kai Zheng,[1] Ting Xie,[1] Rui-Rui Huang,[1] Jie Qin,[*1] Jian-Ping Ma[*2] and Li-Hong Ding[3]

[1] *School of Life Sciences, Shandong University of Technology, Zibo 255049, P. R. China*

[2] *College of Chemistry, Chemical Engineering and Materials Science, Shandong Normal University, Jinan 250014, P. R. China*

[3] *Lanzhou University of Arts and Sciences, Lanzhou, 730000, P. R. China*

** Corresponding author: E-mail: qinjietutu@163.com xxgk123@163.com; Tel.: 0086-533-2780271; Fax: 0086-533-2781329*

Received: 12-17-2019

† These authors contributed equally to this work.

Abstract

Two coordination polymers, namely $[Ag_2(\mathbf{L})(SO_3CF_3)(H_2O)](SO_3CF_3)\bullet CH_2Cl_2$ (**1**) and $[Ag_5(\mathbf{L})_4(H_2O)_2](SbF_6)_5\bullet 5THF$ (**2**), were obtained by reacting oxadiazole-containing tri-armed ligand 1,3,5-tri(2-methylthio-1,3,4-oxadiazole-5yl) benzene (**L**) and silver salts in CH_2Cl_2/THF medium. The two complexes crystallized in the tetragonal space group $I4_1/a$ and orthorhombic space group *Fdd*2, respectively. The Single-crystal X-ray diffraction revealed that the two complexes exhibit strikingly different 3D polymeric structures, which can be ascribed to the different counter anions. **L** in compound **1** acted as a hexa-dentate ligand, binding to two types of Ag^+ atoms to form a 3D polymeric structure. **L** in compound **2** acted as a hexa- and penta-dentate ligand, binding to three types of Ag^+ atoms to form the 3D polymeric structure. The antibacterial activity of the complexes was also investigated.

Keywords: Coordination polymers; oxadiazole-containing spacer; counter anions; antibacterial activity

1. Introduction

The design and synthesis of coordination polymers exhibiting intriguing structures and properties have attracted much attention because of their potential application in catalysis,[1–3] magnetic properties,[4–6] gas adsorption and separation,[7,8] molecular sensing and luminescent materials.[9,10] Many factors, including the nature of the metal ion, design of the organic ligand, auxiliary ligand, solvent medium, and inorganic counter anions can affect the self-assembly process of coordination compounds.[11] Our research group has initiated a synthetic program for the construction of coordination polymers generated from oxadiazole-containing organic ligands.[11,12–14] As an extension of previous studies, we expand oxadiazole-bridging double-armed ligands to the oxadiazole-containing tri-armed ligand **L**, namely 1,3,5-tri(2-methylthio-1,3,4-oxadiazole-5-yl)benzene (Scheme 1). **L** has three arms, each

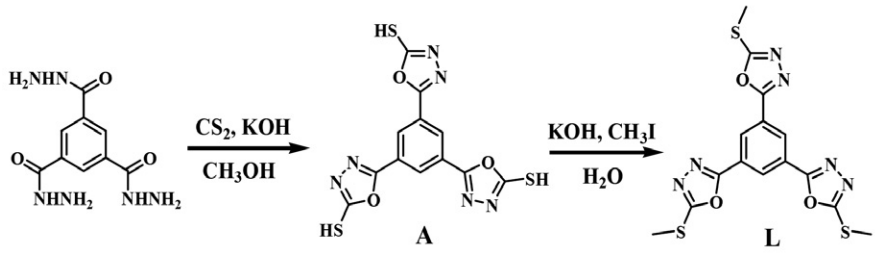

Scheme 1. Synthesis of **L**.

comprising 2-methylthio-1,3,4-oxadiazole. As is known, N atoms on the 1,3,4-oxadiazole ring can bind to transition metals, and the S atom also has strong binding ability to soft metals (e.g., Ag^+). Therefore, **L** can act as a multi-connector in the assembly of complexes with six oxadiazole N-donors and three S-donors, which may result in polynuclear or high-dimensional intricate structures. The reactions of **L** with $AgSO_3CF_3$ and $AgSbF_6$ in CH_2Cl_2/THF allow for two 3D coordination polymers, $[Ag_2(\mathbf{L})(SO_3CF_3)(H_2O)](SO_3CF_3)\bullet CH_2Cl_2$ (**1**) and $[Ag_5(L)_4(H_2O)_2](SbF_6)_5\bullet 5THF$ (**2**), respectively. Here, we report the synthesis and crystal structures of these compounds. Moreover, the antibacterial activities of **1** and **2** were investigated.

2. Experimental

2. 1. Physical Measurements and Materials

Reagents and solvents were purchased commercially from Xiya Reagent. The reagents used in the experiment were all analytical pure, and no further purification was carried out without explanation. The intermediate **A** was synthesized according to the literature method.[11] Infrared spectra in the range of (400–4000 cm^{-1}) were determined by Vector22 Bruker spectrophotometer using potassium bromide tablets. The IR spectra of the synthesized compounds are given in Figure S1 of the supporting information. ^1H NMR spectra were measured on a Bruker AM 500 spectrometer.

2. 2. Synthesis of L

KOH (0.2 g, 3.57 mmol) was added to a solution of **A** (0.4 g, 1.00 mmol) in water (30 mL), the mixture was stirred for 20 minutes at ambient temperature. Then CH_3I (0.8 mL) was added, the mixture was stirred for 6 hours at 0 °C, then filtered. The product was collected and purified on silica gel by column using CH_2Cl_2/THF (5 : 1, v/v) as the eluent to afford **L** as the white crystalline solid (0.34 g). Yield 80 %. M.p. = 134~136 °C, IR (KBr pellet cm^{-1}): 3047(w), 2936(m), 1543(m), 1465(vs), 1432(s), 1323(m), 1181(vs), 1105(m), 947(s), 898(m), 781(s), 731(m), 705(s), 678(m). ^1H NMR (300MHz, $CDCl_3$, 25°C, TMS, ppm): 8.77(s, 3H, $-C_6H_3$), 2.87(s, 9H, $-CH_3$). Single crystals suitable for X-ray crystallographic analysis were grown by slow diffusion of ethanol into dicholmethane solution of **L**.

2. 3. Synthesis of 1

A solution of $AgSO_3CF_3$ (19.6 mg, 0.076 mmol) in THF (10 mL) was layered carefully onto a solution of **L** (10 mg, 0.024 mmol) in CH_2Cl_2. The solutions were left at room temperature for about 1 week, and blocky colorless crystals were obtained. Yield: 55% (based on **L**). IR (KBr pellet cm^{-1}): 2939(w), 1624(m), 1554(m), 1464(vs), 1432(m), 1257(vs), 1181(vs), 1033(s), 974(m), 782(m), 730(m), 678(s), 517(m).

2. 4. Synthesis of 2

A solution of $AgSbF_6$ (26.6 mg, 0.077 mmol) in THF (10 mL) was layered carefully onto a solution of **L** (10 mg, 0.024 mmol) in CH_2Cl_2. The solutions were left at room temperature for about 2 weeks, and claviform colorless crystals were obtained. Yield: 40% (based on **L**). IR (KBr pellet cm^{-1}): 2936(w), 1621(m), 1552(m), 1464(vs), 1431(m), 1182(s), 1105(w), 976(w), 784(m), 663(vs).

Table 1. Crystallographic data for **L**, **1**, and **2**.

	L	**1**	**2**
Empirical formula	$C_{16}H_{14}Cl_2N_6O_3S_3$	$C_{18}H_{16}Ag_2C_{l2}F_6N_6O_{10}S_5$	$C_{80}H_{92}Ag_5F_{30}N_{24}O_{19}S_{12}Sb_5$
Mr	505.41	1037.31	3796.60
Crystal System	triclinic	tetragonal	orthorhombic
Space group	*P*-1	$I4_1/a$	*Fdd*2
a (Å)	12.3957(15)	29.635(2)	23.442(3)
b (Å)	13.1933(16)	29.635(2)	49.277(8)
c (Å)	14.4155(18)	15.200(2)	22.284(3)
α (°)	111.293(2)	90.00	90.00
β (°)	106.666(2)	90.00	90.00
γ(°)	94.493(2)	90.00	90.00
V ($Å^3$)	2059.9(4)	13350(2)	25741(6)
Z	4	4	8
ρ_c (g cm^{-3})	1.630	2.064	1.959
F(000)	1032	8228	14752.0
T / K	173(2)	173(2)	173(2)
μ(Mo-Kα)/ mm^{-1}	0.652	1.738	2.079
GOF (F^2)	1.021	1.098	1.029
Data / restraints / parameters	7495 / 0 / 547	5907 / 16 / 474	11022 / 19 / 740
R_1[a], wR_2[b] ($I>2\sigma(I)$)	0.0421, 0.1046	0.0493, 0.1046	0.0452, 0.1114

[a] $R_1 = \Sigma||F_o| - |F_c||/\Sigma|F_o|$. [b] $wR_2 = [\Sigma w(F_o^2 - F_c^2)^2/\Sigma w(F_o^2)]^{1/2}$

2. 5. Determination of Crystal Structures

The single crystal of the synthesized compounds were measured using Bruker Smart Apex CCD diffractometer. The collected data were reduced using SAINT,[15] and multi-scan absorption corrections were performed using SADABS.[16] The structures were solved by direct methods and refined against F^2 by full-matrix least-squares.[17] All of the non-hydrogen atoms were refined aniso-tropically. All the hydrogen atoms were generated geometrically and refined isotropically using the riding model except the hydrogen atoms of water molecules, which were located directly from the Fourier map. Details of crystallographic parameters, data collection, and refinements are summarized in Table 1. The bond length and bond angle of the crystals are shown in Tables 2 and 3.

Table 2. Selected bond distances (Å) and angles (°) for complex **1**.

Ag1-N2$^{\#1}$	2.274(4)	Ag1-N4$^{\#2}$	2.293(4)
Ag1-N1	2.316(4)	Ag1-N3$^{\#3}$	2.311(4)
Ag2-N5	2.229(4)	Ag2-N6$^{\#4}$	2.282(4)
Ag2-O4	2.566(4)	Ag2-O7	2.322(4)
N2$^{\#1}$-Ag1-N4$^{\#2}$	114.42(14)	O7-Ag2-O4	93.19(16)
N2$^{\#1}$-Ag1-N3$^{\#3}$	106.15(14)	N5-Ag2-N6$^{\#4}$	138.06(14)
N4$^{\#2}$-Ag1-N3$^{\#3}$	106.39(15)	N5-Ag2-O7	119.72(16)
N2$^{\#1}$-Ag1-N1	113.64(14)	N6$^{\#4}$-Ag2-O7	94.29(15)
N4$^{\#2}$-Ag1-N1	101.77(15)	N5-Ag2-O4	87.70(14)
N3$^{\#3}$-Ag1-N1	114.46(14)	N6$^{\#4}$-Ag2-O4	116.05(14)
Ag1-N2$^{\#1}$	2.274(4)	Ag1-N4$^{\#2}$	2.293(4)
Ag1-N1	2.316(4)	Ag1-N3$^{\#3}$	2.311(4)
Ag2-N5	2.229(4)	Ag2-N6$^{\#4}$	2.282(4)

Symmetry code: #1: -y+7/4, x+1/4, z+1/4; #2: y-1/4, -x+7/4, z+3/4 ; #3: -x+3/2, -y+2, z+1/2; #4: -y+7/4, :x+1/4, z-3/4

Table 3 Selected bond distances (Å) and angles (°) for complex **2**.

Ag1-N2	2.257(5)	Ag1-N2$^{\#1}$	2.257(5)
Ag1-N9	2.328(6)	Ag1-N9$^{\#1}$	2.328(6)
Ag2-N7	2.294(6)	Ag2-N4$^{\#2}$	2.374(6)
Ag2-N11$^{\#2}$	2.325(6)	Ag2-O7	2.466(6)
Ag2-S1$^{\#3}$	2.9549(19)	Ag3-N1	2.362(6)
Ag3-N10	2.325(7)	Ag3-N12$^{\#1}$	2.384(6)
Ag3-N6$^{\#4}$	2.413(7)	Ag3-N3$^{\#1}$	2.548(6)
N2$^{\#1}$-Ag1-N2	108.5(3)	N2$^{\#1}$-Ag1-N9$^{\#1}$	123.1(2)
N2-Ag(1)-N9$^{\#1}$	109.6(2)	N2$^{\#1}$-Ag1-N9	109.6(2)
N2-Ag1-N9	123.1(2)	N9$^{\#1}$-Ag1-N9	82.1(3)
N7-Ag2-N4$^{\#2}$	92.6(2)	N1$^{\#2}$-Ag2-N4$^{\#2}$	134.8(2)
N7-Ag2-N11$^{\#2}$	129.3(2)	O7-Ag2-S1$^{\#3}$	178.13(17)
N10-Ag3-N1	110.7(2)	N10-Ag3-^{N6}#4	82.7(2)
N10-Ag3-N12$^{\#1}$	94.8(2)	N10-Ag3-N3$^{\#1}$	132.2(2)
N6$^{\#4}$-Ag3-N12$^{\#1}$	114.5(2)	N12$^{\#1}$-Ag3-N3$^{\#1}$	132.76(19)
N3$^{\#1}$-Ag3-N1	79.2(2)	N1-Ag3-N6$^{\#4}$	152.4(2)

Symmetry code: #1: -x+3/2, -y+3/2, z; #2: -x+1, -y+3/2, z+1/2; #3: x-1/2, y, z+1/2; #4:-x+7/4, y-1/4, z+1/4.

2. 6. Antibacterial Activity Test

Four referenced bacterial strains, *B. subtilis*, *E. coli*, *P. aeruginosa* and *S. aureus* were selected. Streptomycin was used as a positive control. The IC_{50} (half minimum inhibitory concentrations) of the test compounds were determined by a colorimetric method using the dye MTT (3-(4,5-dimethylth-iazol-2-yl)-2,5-diphenyl tetrazolium-bromide). Stock solutions of the synthesized compounds (100 μg/mL) were prepared in DMSO, and sequentially diluted with Mueller-Hinton medium. The antibacterial activities were evaluated by the method reported before.[18] The procedure of antibacterial activity was given in detail in *Supporting Information.*

3. Results and Discussion

3. 1. Crystal Structure Analysis

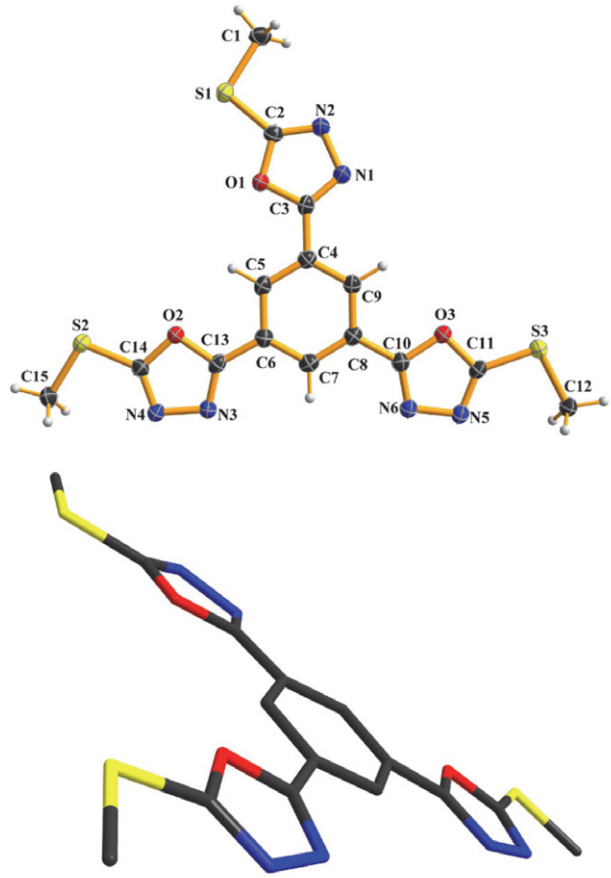

Figure 1. Molecular structure of **L** (50% probability displacement ellipsoids), front and side views are presented.

Colorless crystals of **L** suitable for X-ray structure analysis were obtained via the slow diffusion of ethanol into a dicholmethane solution of **L**. **L** crystallized in the triclinic space group $P\bar{1}$; there are two L and two CH_2Cl_2

molecules in the asymmetric unit. As shown in Figure 1, **L** has an approximately planar structure except for the methyl H atoms stretching out of the plane. The dihedral angles between the central benzene ring and surrounding oxadiazole rings are 4.371(7)°, 6.136(2)°, and 7.257(2)°, respectively.

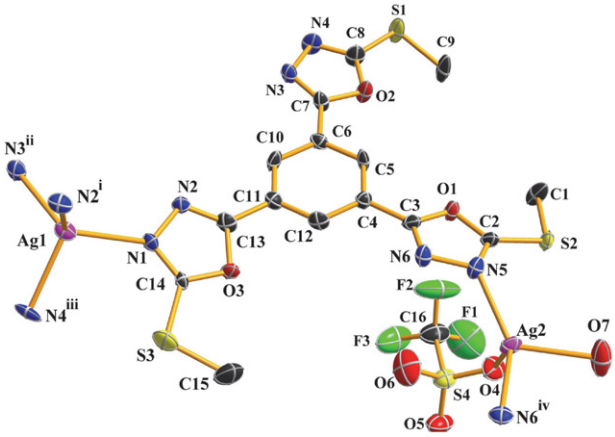

Figure 2. The coordination environment of Ag^+ in **1** at 50% probability displacement. (Solvent molecules are omitted for clarity) Symmetry codes: (i) -y+7/4, x+1/4, z+1/4; (ii) -x+3/2, -y+2, z+1/2; (iii) y-1/4, -x+7/4, z+3/4; (iv) -y+7/4, x+1/4, z-3/4.

Crystallization of **L** with $AgSO_3CF_3$ in a CH_2Cl_2/THF mixed-solvent system at room temperature produced complex **1** with a 55% yield. **1** crystallized in the tetragonal space group $I4_1/a$. Single crystal analysis revealed that two crystallographically independent Ag^+ ions, one ligand **L**, one coordinated water molecule, one coordinated $CF_3SO_3^-$anion, one free $CF_3SO_3^-$anion and one solvent CH_2Cl_2 molecule compose the asymmetric unit of **1**. After complexation, **L** was no longer planar in complex **1**, which was evident from the dihedral angles between the central benzene ring and surrounding oxadiazole rings being 11.004(7)°, 16.914(8)°, and 21.110(5)°, respectively. As illustrated in Figure 2, the Ag1 and Ag2 coordination environments are distinct from each other. The Ag1 center adopts a distorted tetrahedral coordination sphere, which consists of four $N_{oxadiazole}$ donors (N1, N2i, $N3^{ii}$, and $N4^{iii}$) from four separate ligands. Ag2 is also four-coordinated by two $N_{oxadiazole}$ atoms (N5 and $N6^{iv}$) along with O atoms from a water molecule (O7) and $CF_3SO_3^-$anion (O4). The Ag1-N bond lengths are in the range of 2.274(4)–2.316(4) Å, which are longer than the bond lengths of Ag2-N (2.229(4)–2.282(4)) The Ag-N and Ag-O bond lengths are in agreement with those values in a previous report.[14]

In the extended structure, neighboring Ag1 centers are bridged by four $N_{oxadiazole}$ atoms into a $\{Ag_2N_4\}$ dinuclear core (Ag1···Ag1 distance of 3.8158(7) Å), which is similar to that found in compounds generated from oxadiazole-bridging double-armed ligands.[14] Notably, the two adjacent $\{Ag_2N_4\}$ dinuclear units are almost perpendicular to each other (dihedral angle of 89.923°) and are arranged

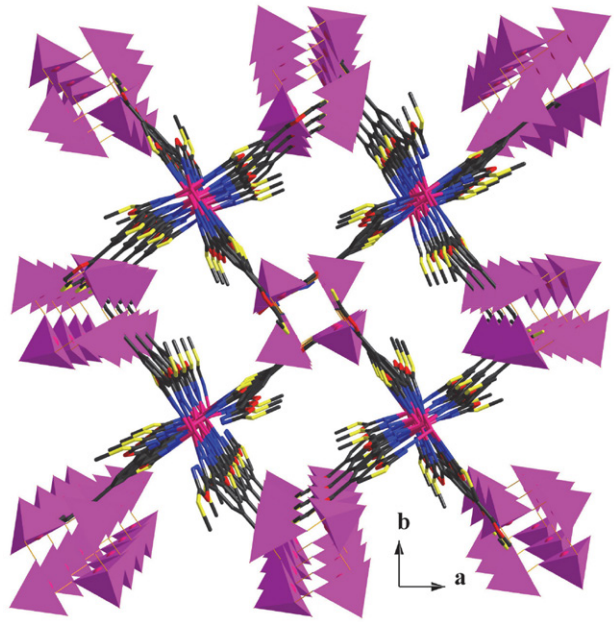

Figure 4. 3D framework of **1** (anions and CH_2Cl_2 molecules are omitted for clarity), and Ag2 centers are highlighted as fuchsia polyhedrons.

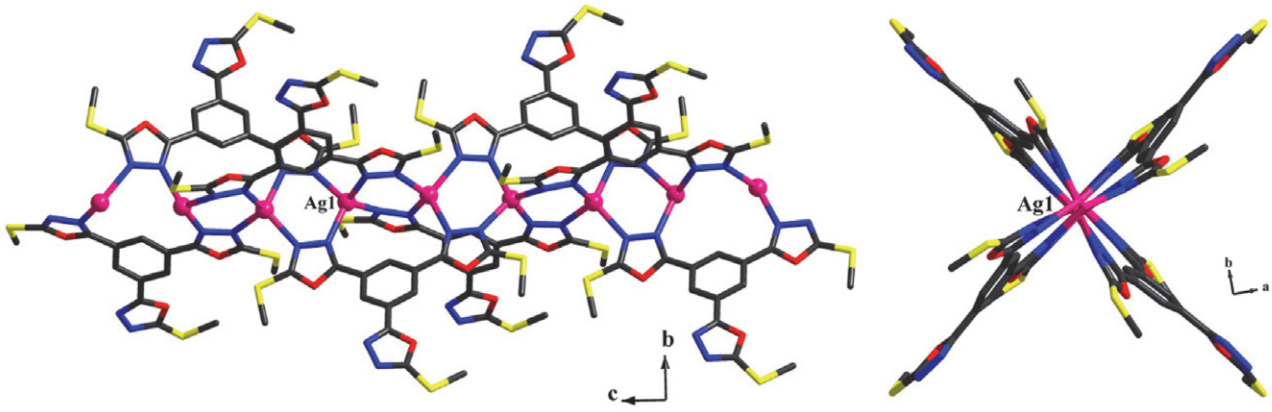

Figure 3. 1D chain structure consists of Ag1 in **1**.

alternately to form a 1D polymeric chain extending along the crystallographic *c* axis (Figure 3).

The remaining oxadiazole groups on these $\{Ag_2N_4\}_n$ chains adopt a μ_2-η^1:η^1 bridging mode, connecting four Ag2 centers to form a twelve-membered $\{Ag_4N_8\}$ saddle-like ring (Figure S2). In the solid state, these $\{Ag_4N_8\}$ clusters are located between the $\{Ag_2N_4\}_n$ chains, and further link the 1D chains into a 3D microporous supramolecular network with rectangular channels along the *c* axis (Figure 4). The $CF_3SO_3^-$ anions and solvent CH_2Cl_2 molecules are present in the channels. In summary, each **L** in compound **1** acts as a hexa-dentate ligand, binding to six Ag^+ atoms, in which all the $N_{oxadiazole}$ donors are utilized to bind Ag^+ ions into a 3D polymeric structure, whereas $S_{methylthio}$ donors are not involved in coordination.

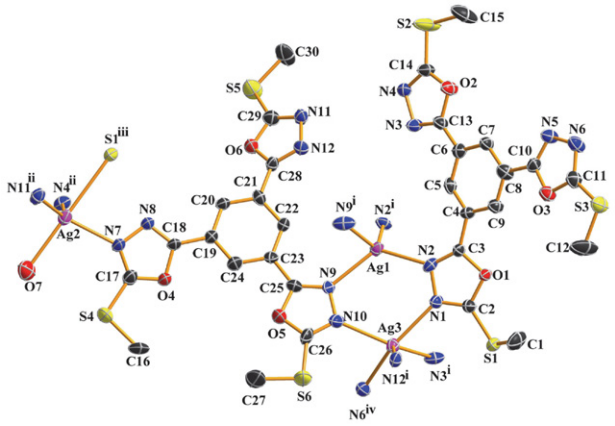

Figure 5. The coordination environment of Ag^+ in **2** at 50% probability displacement. (Anions and solvent molecules are omitted for clarity) Symmetry codes: (i) -x+3/2, -y+3/2, z; (ii) -x+1, -y+3/2, z+1/2; (iii) x-1/2, y, z+1/2; (iv) -x+7/4, y-1/4, z+1/4.

To investigate the effect of the counter anions on the structural motif of the{Ag^+-**L**} coordination system, the weakly coordinated SbF6$^-$ anion was used instead of the strongly coordinated $CF_3SO_3^-$ anion for the self-assembly reaction in the same CH_2Cl_2/THF solvent system; this produced compound **2** with a 40% yield. Single crystal analysis revealed that five crystallographically independent Ag^+ ions, four ligands, two coordinated water molecules, five free SbF_6^-anions, and five tetrahydrofuran molecules constitute the asymmetric unit of **2**. In complex **2**, the dihedral angles between the central benzene ring and surrounding oxadiazole rings exhibit a large difference. For the central benzene ring involving C4–C9, the dihedral angles are 0.771(2))°, 8.022(4))°, and 23.962(6))°, respectively. For the central benzene ring involving C19–C24, the dihedral angles are 4.827(6))°, 18.136(8))°, and 31.515(8))°, respectively.

There are three independent Ag^+ centers in **2** (Figure 5). The first center, Ag1, is located in a distorted tetrahedral coordination sphere with four $N_{oxadiazole}$ donors (N2, N9, N2^i, and N9^i). The Ag1-N bond lengths are 2.257(5)–2.328(6) Å. Ag2 is five-coordinated by three $N_{oxadiazole}$ donors (N7, N4^{ii}, and N11^{ii}), one S atom and one O atom from a water molecule. The Addison distortion index, τ, (τ = (β – α)/60, where α and β are the two largest coordinated angles in the complex; perfect square pyramidal, τ = 0; perfect trigonal bipyramidal, τ = 1),[19] for Ag2 is 0.72, indicating a distorted trigonal bipyramidal coordination sphere. The axial O7-Ag2-S1^{iii} angle of 178.13(17)° is slightly smaller than the ideal value of 180°. The equatorial Ag2-N bond lengths are 2.325(6)–2.374(6) Å, while the axial Ag2-O7 and Ag2-S1^{iii} distances are 2.466(6) and 2.9549(19) Å, respectively; thus, it is an elongated trigonal bipyramidal structure. Ag3 is also five-coordinated, with a

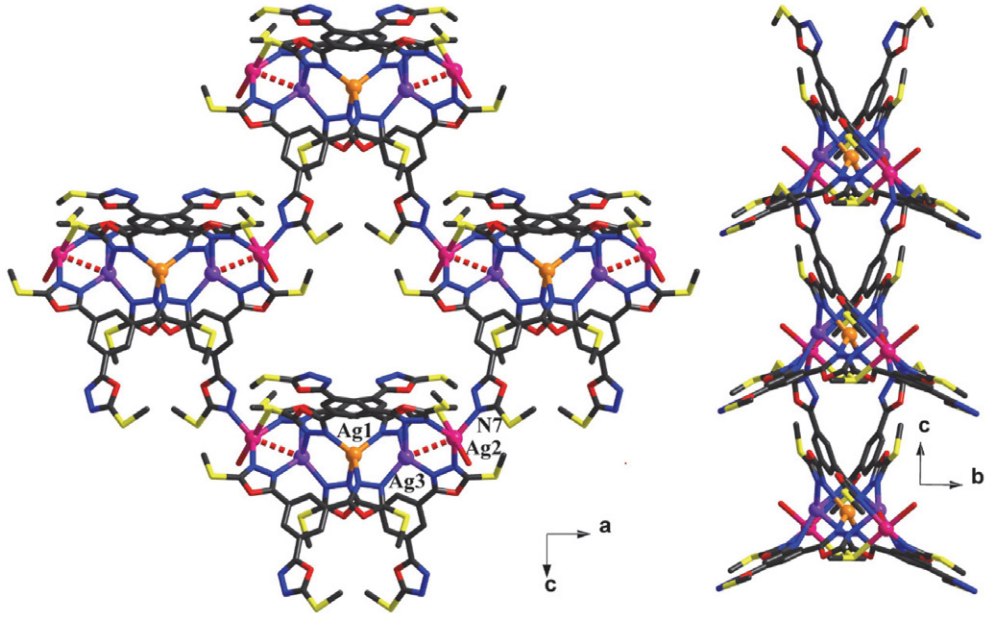

Figure 6. View of 2D network in **2**, front and side views are presented.

τ of 0.33. Therefore, Ag3 is best described as distorted square pyramidal with N10 in axial positions and the other N donors (N1, N3^{i}, N6^{iv}, and N12^{i}) forming the equatorial plane. The bond angles around the Ag^{+} center range from 79.2(2) to 152.4(2)° in the equatorial positions and from82.7(2) to 132.2(2)° for the apical positions. Ag3-N bond lengths are 2.325(7)–2.548(6) Å, which is the longest among these Ag-N bonds.

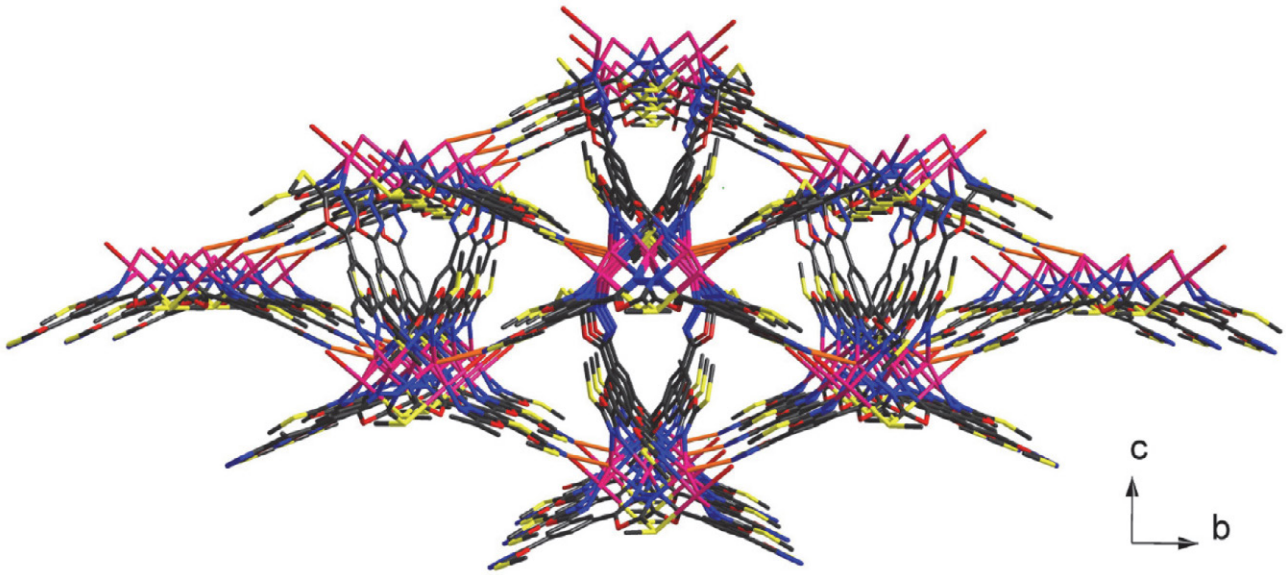

Figure 7. View of 3D network of **2** along *a* axis (anions and THF molecules are omitted for clarity).

The $\{Ag_2N_4\}$ dinuclear moieties were also found in compound **2**. The shortest Ag2···Ag3 distance is 3.2013(8) Å (while the Ag3···Ag1 separation is 3.713(1) Å), indicating weak Ag···Ag interactions. In the solid state, four $\{Ag_2N_4\}$ units are interlocked together into a butterfly-like penta-nuclear sub-building block (as shown in Figure S3). These sub-building blocks are strung together by the Ag2-N7 bond into a two-dimensional sheet extending in the crystallographic *ac* plane, as shown in Figure 6. These 2D layers are further connected by Ag3-N6 linkages into a three-dimensional network with triangular channels along the crystallographic *a* axis, in which uncoordinated SbF_6^- counteranions and THF guest molecules are located in place of CH_2Cl_2 (Figure 7). Principally, one of the **L** ligand in compound **2** acts as a hexa-dentate ligand, binding to six Ag^{+} *via* N1, N2, N3, N4, N6, and S1, while the other ligand acts as a penta-dentate ligand, binding to five Ag^{+} *via* N7, N9, N10, N11, and N12.

3. 2. Antibacterial Activity

Among the diverse transition metals, silver has fundamental importance in bioinorganic chemistry, and the use of silver metal complexes for medicinal applications has been well documented.[20,21] Silver-based complexes have been used as antimicrobials since the successful use of silver-containing creams for burn treatment.[22] We have reported the antibacterial activities of silver complexes based on quinoline or hydrazone scaffolds.[18,23,24] As a continuation of our efforts in exploring new antibacterial reagents to supplement structure–activity information, the *in vitro* antibacterial activities of the synthesized compounds were assessed. The IC_{50} (half minimum inhibitory concentrations) values of the test compounds are presented in Table 4. Known antibiotic, such as streptomycin, was used as control drug.

Table 4 Antimicrobial activity of the tested compounds.

Compounds	***Half maximal inhibitory concentrations* (*μg*/mL)**			
	Gram-negative		**Gram-positive**	
	E.coli	***P.aeruginosa***	***B.subtilis***	***S.aureus***
L	>50	>50	>50	>50
1	8.62	9.35	13.41	10.41
2	9.43	7.56	15.23	6.74
$AgSO_3CF_3$	3.53	3.27	8.21	4.67
$AgSbF_6$	2.03	0.19	7.02	3.87
Streptomycin	3.94	>50	4.12	5.24

As shown in Table 4, against all the tested bacteria, the free ligand **L** was inactive under the tested conditions. However, the introduction of Ag^{+} on the ligand resulted in improved antibacterial activity, especially against the tested gram-negative strains, with IC_{50} values of 7.56 to 9.43 μg mL^{-1}. For the tested gram-negative strains, the IC_{50} values ranged from6.74 to 15.23 μg mL^{-1}. It is evident that the

activity of the two complexes is dependent primarily on the presence of the Ag^+ ion. It has been found that the nature of ligands, chelate effect of ligands, nuclearity, and total charge are the main factors contributing to the biological activity of the Ag-compounds.[25] Compared with our previously reported quinoline-silver(I) complexes and hydrazone-silver(I) complexes, the bioactivities of **1** and **2** are slightly lower. This can be attributed to the lack of a chelate effect because the $N_{oxadiazole}$ donors of **L** in **1** and **2** are all in the bridging mode.

4. Conclusions

In conclusion, we synthesized and characterized two novel 3D Ag(I) coordination polymers generated from the oxadiazole-containing tri-armed ligand **L**. Complexes **1** and **2** are both three-dimensional frameworks, but **L** features different coordination modes in them. **L** in complex **1** acts as a hexa-dentate ligand (binding to six Ag^+ atoms *via* all the N donors), while in **2**, one of the ligands acts as a hexa-dentate ligand (binding to six Ag^+ atoms *via* five N donors and one S donor), and the other **L** acts as a peta-dentate ligand (binding to five Ag^+ *via* five N donors). The structural diversity reveals that inorganic counter anions play an important role in building up the coordination framework. In addition, complexes **1** and **2** exhibited potent antibacterial activity.

5. References

1. E. G. R. de Arruda, M. A. de Farias, S. A. V. Jannuzzi, S. D. A. Gonsales, R. A. Timm, S. Sharma, G. Zoppellaro, L. T. Kubota, M. Knobel, A. L. B. Formiga, *Inorg. Chim. Acta* **2017**, *466*, 456–463. **DOI:**10.1016/j.ica.2017.06.073
2. A. Rühling, H. J. Galla, F. Glorius, *Chem. Eur. J.* **2015**, *21*, 12291–12294. **DOI:**10.1002/chem.201502542
3. J. Rodriguez, D. Bourissou, *Angew. Chem. Int. Ed.* **2018**, *57*, 386–388. **DOI:**10.1002/anie.201710105
4. T. P. Latendresse, V. Vieru, B. O. Wilkins, N. S. Bhuvanesh, L. F. Chibotaru, M. Nippe, *Angew. Chem. Int. Ed*. 2018, 57,8164–8169. **DOI:**10.1002/anie.201804075
5. M. B. Coban, E. Gungor, H. Kara, U. Baisch, Y. Acar, *J. Mol. Struct.* **2018**, *1154*, 579–586. **DOI:**10.1016/j.molstruc.2017.10.049
6. A. T. Baryshnikova, B. F. Minaev, G. V. Baryshnikov, H. Ågren, *Inorg. Chim. Acta* **2019**, *485*, 73–79. **DOI:**10.1016/j.ica.2018.09.086
7. I. Ahmed, S. H. Jhung, *Chem. Eng. J.* **2017**, *310*, 197–215. **DOI:**10.1016/j.cej.2016.10.115
8. Y. Y. Jia, X. T. Liu, R. Feng, S. Y. Zhang, P. Zhang, Y. B. He, Y. H. Zha-ng, X. H. Bu, *Inorg. Chem. Front* **2016**, *3*, 1510–1515. **DOI:**10.1039/C6QI00191B
9. W. P. Lustig, S. Mukherjee, N. D. Rudd, A. V. Desai, J. Li, S. K. Ghosh, *Chem. Soc. Rev.* **2017**, *46*, 3242–3285. **DOI:**10.1039/C6CS00930A
10. M. Gon, K. Tanaka, Y. Chujo, *Bull. Chem. Soc. Jpn*. **2019**, *92*, 7–18. **DOI:**10.1246/bcsj.20180245
11. L. N. Wang, L. Fu, J. W. Zhu, Y. Xu, M. Zhang, Q. You, P. Wang, J. Qin, *Acta Chim. Slov.* **2017**, *64*, 202–207. **DOI:** 10.17344/acsi.2016.3109
12. C. W. Zhao, J. P. Ma, Q. K. Liu, X. R. Wang, Y. Liu, J. Yang, J. S. Yang, Y. B. Dong, *Chem. Commun*. **2016**, *52*, 5238–5241. **DOI:**10.1039/C6CC00189K
13. Y. B. Dong, Q. Zhang, L. L. Liu, J. P. Ma, B. Tang, R. Q. Huang, *J. Am. Chem. Soc.* **2007**, *129*, 1514–1515. **DOI:**10.1021/ja067384z
14. Y. B. Dong, H. X. Xu, J. P. Ma, R. Q. Huang, *Inorg. Chem.* **2006**, *45*, 3325–3343. **DOI:**10.1021/ic052158w
15. Bruker, SMART and SAINT. Bruker AXS Inc., Madison, Wisconsin, USA, **2002**.
16. G. M. Sheldrick, SADABS. Program for Empirical Absorp-tion Correction of Area Detector, University of Göttingen, Germany, **1996**.
17. G. M. Sheldrick, *Acta Crystallogr.* **2008**, *A64*, 112–122. **DOI:**10.1107/S0108767307043930
18. L. Zhang, Z. W. Man, Y. Zhang, J. Hong, M. R. Guo, J. Qin, *Acta Chim. Slov.* **2016**, *63*, 891–898. **DOI:**10.17344/acsi.2016.2895
19. A. W. Addison, T. N. Rao. *J. Chem. Soc., Dalton Trans.* **1984**, 1349–1356. **DOI:**10.1039/DT9840001349
20. K. Gholivand, F. Molaei, N. Oroujzadeh, R. Mobasseri, H. Naderi-Manesh, *Inorg. Chim. Acta* **2014**, *423*, 107–116. **DOI:**10.1016/j.ica.2014.07.029
21. J. H. B. Nunes, R. E. F. de Paiva, A. Cuin, W. R. Lustri, P. P. Corbi, *Polyhedron* **2015**, *85*, 437–444. **DOI:**10.1016/j.poly.2014.09.010
22. S. Silver, L. T. Phung, G. Silver, *J. Ind. Microbiol. Biotechnol*., **2006**, *33*, 627–634. **DOI:**10.1007/s10295-006-0139-7
23. S. S. Zhao, P. Wang, L. N. Wang, L. Fu, X. M. Han, J. Qin, S. S. Qian, *J. Coord. Chem.* **2017**, *70*, 885–897. **DOI:**10.1080/00958972.2017.1281915
24. Q. L. Ren, S. S. Zhao, L. X. Song, S. S. Qian, J. Qin, *J. Coord. Chem.* **2016**, *69*, 227–237. **DOI:**10.1080/00958972.2015.1110240
25. M. Zampakou, S. Balala, F. Perdih, S. Kalogiannis, I. Turel, G. Psomas. *RSC Adv.* **2015**, *5*, 11861–11872. **DOI:**10.1039/C4RA11682H

Povzetek

Z reakcijo med triveznim ligandom z oksadiazolom, 1,3,5-tri(2-metiltio-1,3,4-oxadiazol-5il) benzen (**L**), in srebrovimi solmi v mediju CH_2Cl_2/THF smo sintetizirali dva koordinacijska polimera, $[Ag_2(\mathbf{L})(SO_3CF_3)(H_2O)](SO_3CF_3)\bullet CH_2Cl_2$ (**1**) in $[Ag_5(\mathbf{L})_4(H_2O)_2](SbF_6)_5\bullet 5THF$ (**2**). Spojini kristalizirata v tetragonalni prostorski skupini $I4_1/a$ oziroma ortorombski prostorski skupini *Fdd*2. Rentgenska difrakcija na monokristalu je pokazala bistvene razlike med 3D polimernima strukturama obeh spojin, kar lahko pripišemo različnim protiionom. V spojini **1** je ligand **L** šestvezen in koordiniran na dve vrsti Ag^+ ionov s katerimi tvori 3D polimerno strukturo. V spojini **2** je ligand **L** pet- in šestvezen in koordiniran na tri vrste Ag^+ ionov s katerimi prav tako tvori 3D polimerno strukturo. Raziskovali smo tudi protibakterijsko učinkovitost novih koordinacijskih spojin.